

Alfvén Wave Heating Model of an Active Region and Comparisons with EIS Observations

A. Lawless^{1,2}, M. Asgari-Targhi²

¹Trinity College Dublin, ²Harvard-Smithsonian Centre for Astrophysics

Abstract

We study the generation and dissipation of Alfvén waves in open and closed field lines using the images from the Solar Dynamics Observatory's (SDO) Atmospheric Imaging Assembly (AIA). The goal is to search for observational evidence of Alfvén waves in the solar corona and to understand their role in coronal heating. We focus on one particular active region of the 10th December 2007 (see Figure 2). Using the MDI magnetogram and the potential field modelling of this region, we create three-dimensional MHD models for several open and closed field lines in different locations in the active region. For each model we compute the temperature, pressure, magnetic field strength, average heating rate and other parameters along the loop. We then compare these results with the EIS observations.

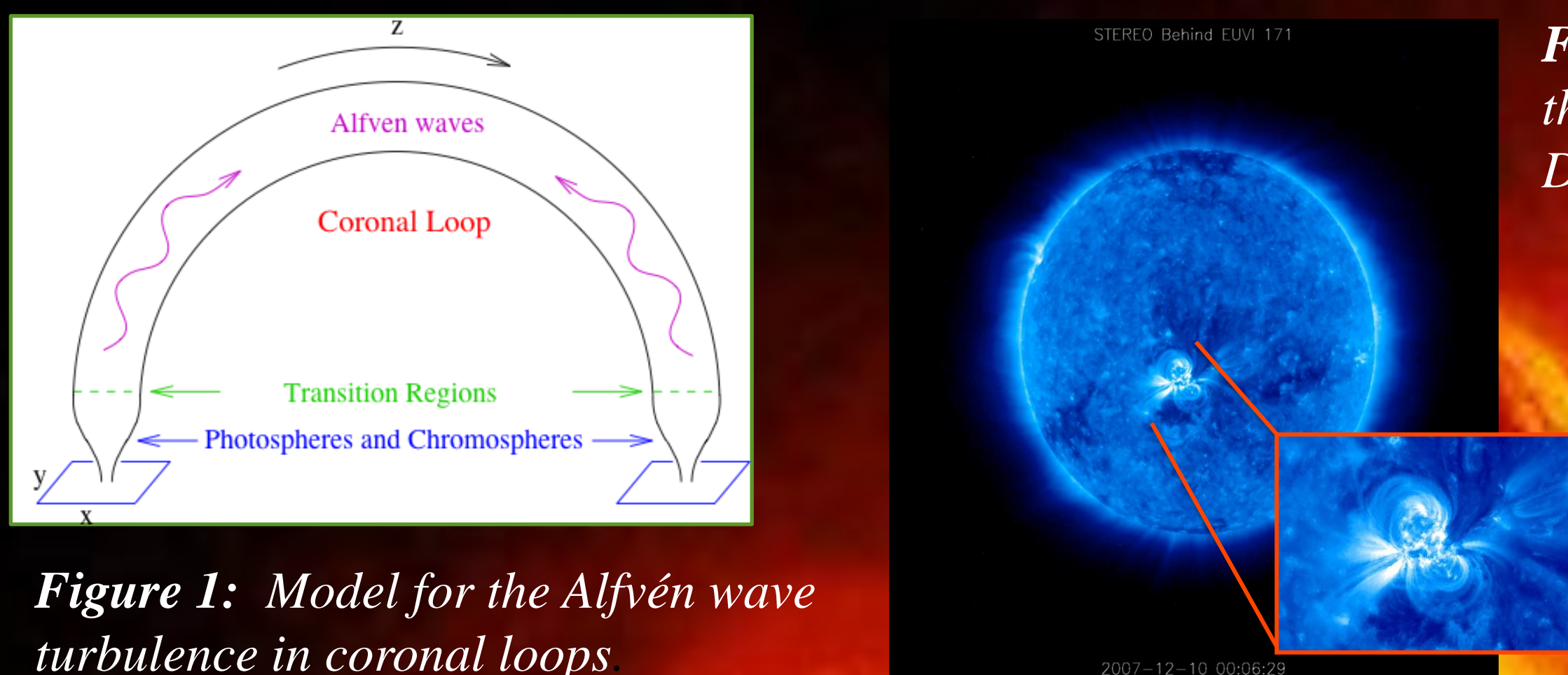


Figure 1: Model for the Alfvén wave turbulence in coronal loops

Background

The Coronal Heating Problem

- The corona has a temperature significantly higher than that of the photosphere.
- Seems to violate the 2nd Law of Thermodynamics.
- Two possible solutions: **Nanoflares** and **Alfvén wave turbulence**

Nanoflares

- Random motions of coronal loop footpoints causes braiding.
- Stress builds up.
- Magnetic field lines break up and reconnect, **releasing energy**.

Alfvén Wave Turbulence

- Random motions of coronal loop footpoints.
- Causes Alfvén waves to propagate along coronal loops.
- Waves meet at centre of loop
- Interact nonlinearly, **releasing energy**.

Aims of this Project

- To conduct comprehensive studies of generation and dissipation of **Alfvén waves** in the solar atmosphere in observed open and closed field lines using **analytical and numerical** tools.
- To **interpret observations and compare** them to the modeling results.

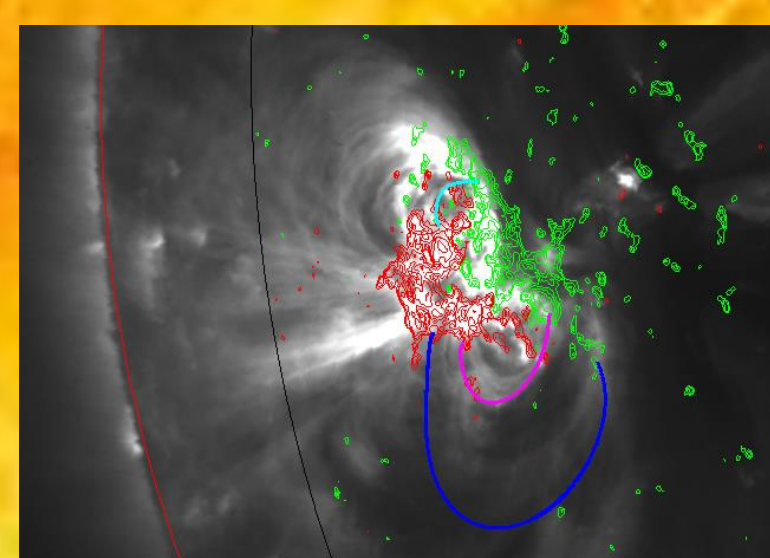
Modeling

- Coronal modelling system program (CMS2) used to select and model a closed loop.
- Fortran program, evolve.f90, used to solve differential equations:

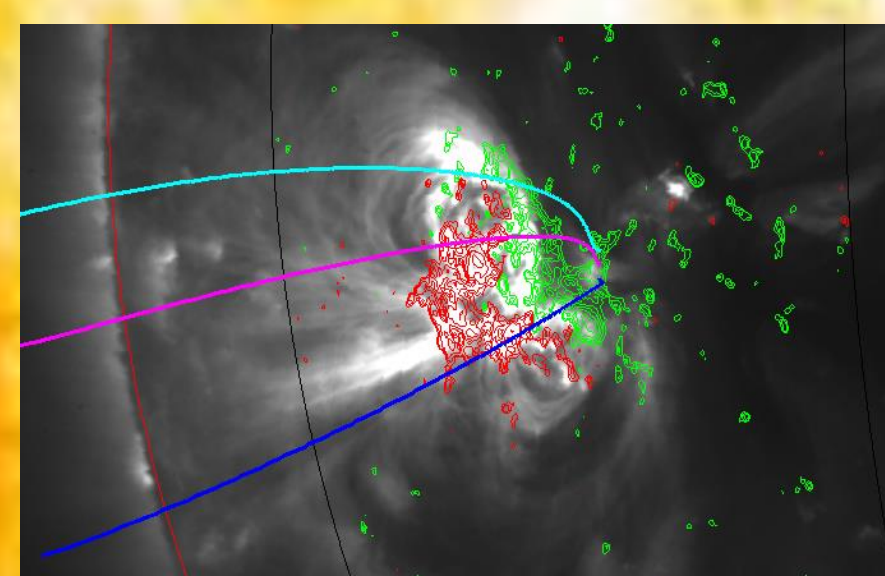
$$\frac{d\mathbf{B}}{dt} \approx \nabla \times (\mathbf{v} \times \mathbf{B}) \quad \rho \frac{D\mathbf{v}}{Dt} = -\nabla p - \rho \mathbf{g} + (\mathbf{j} \times \mathbf{B}) + \mathbf{F}_{\text{visc}}$$

Magnetic Induction Equation Plasma Equation of Motion

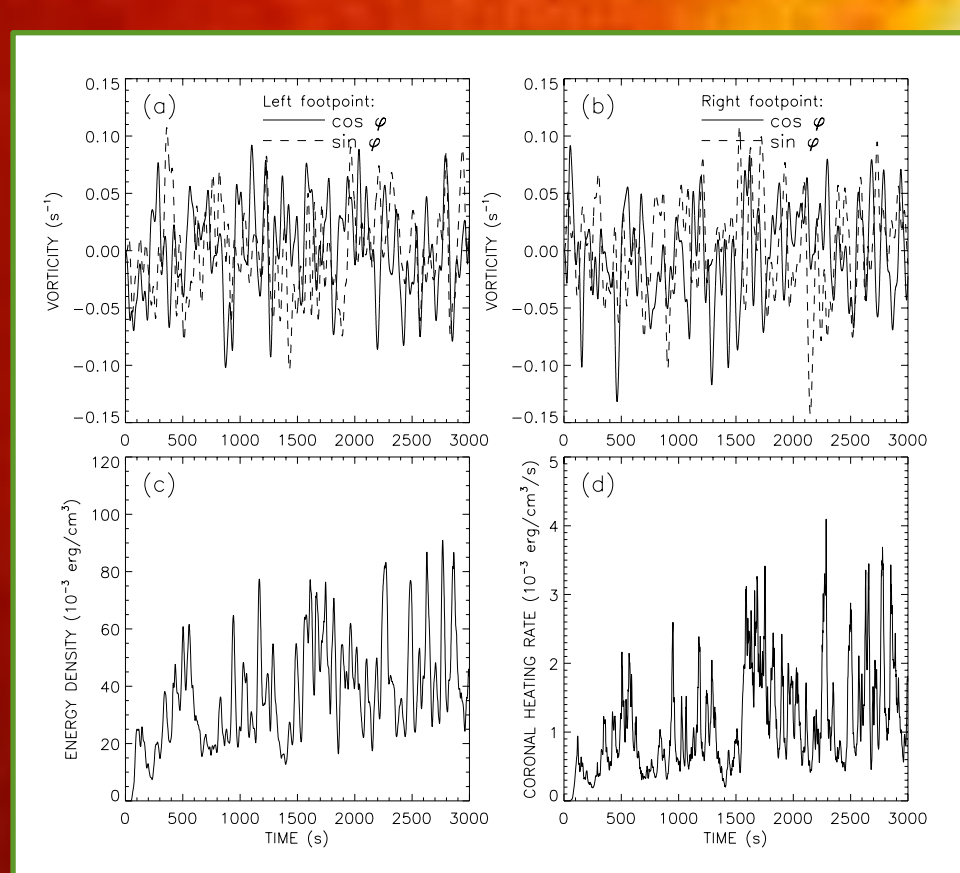
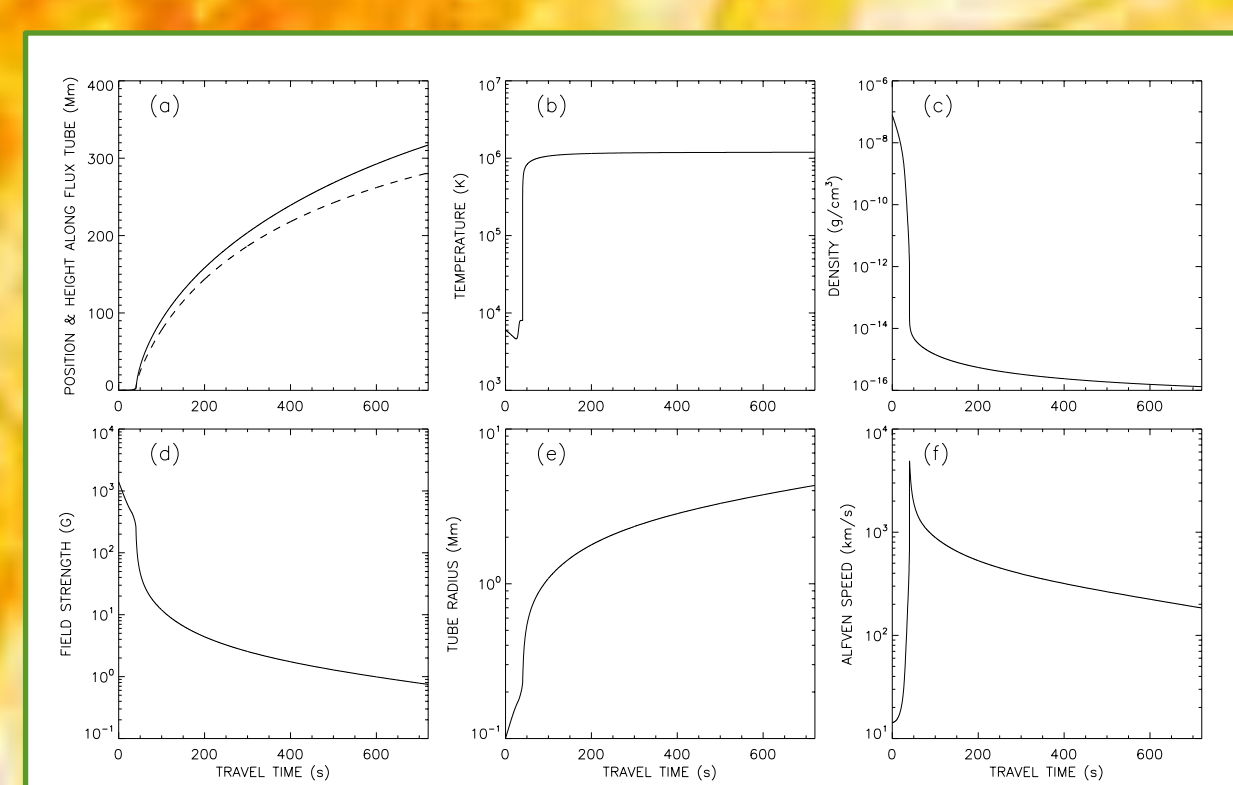
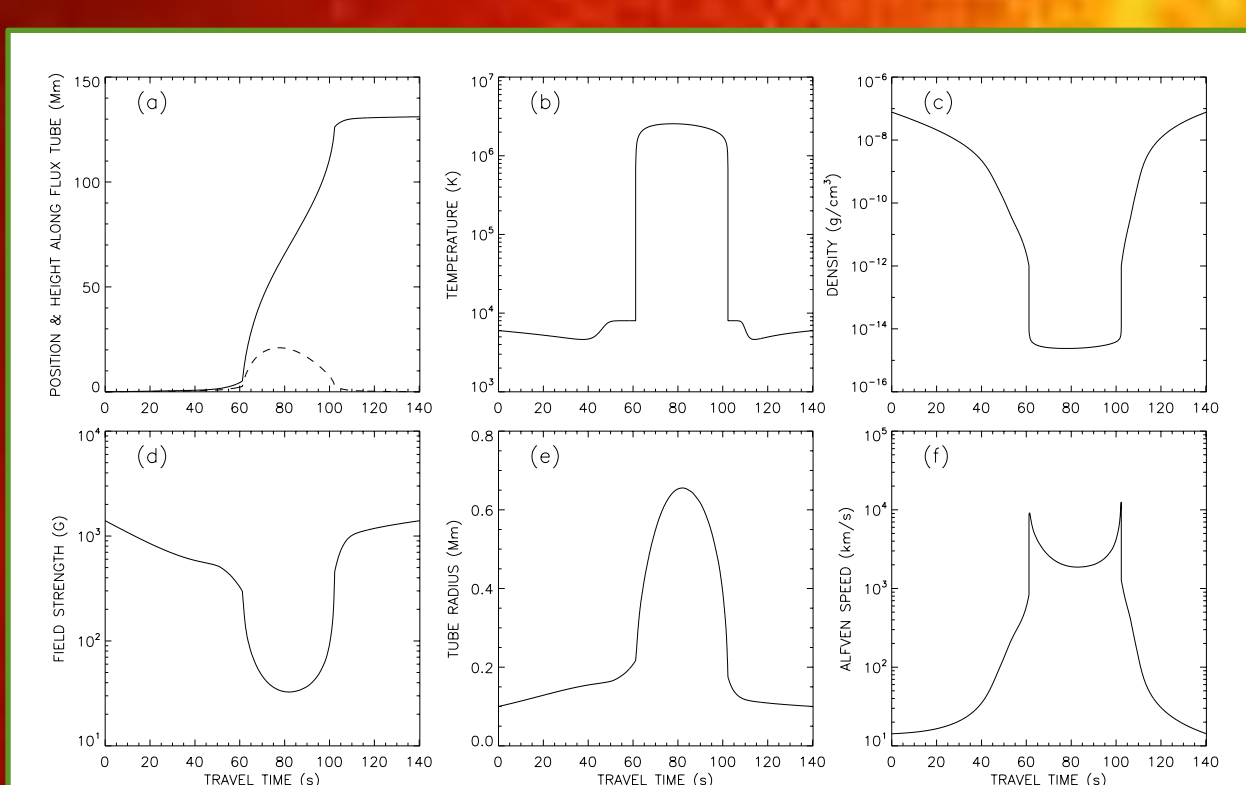
- IDL Braid program used to analyse the results.
- It computes temperature, pressure, magnetic field strength, average heating rate and other parameters along the loop.



Figures 3 & 4: Examples of closed (left) and open (below) loops selected using CMS2



Modeling Results



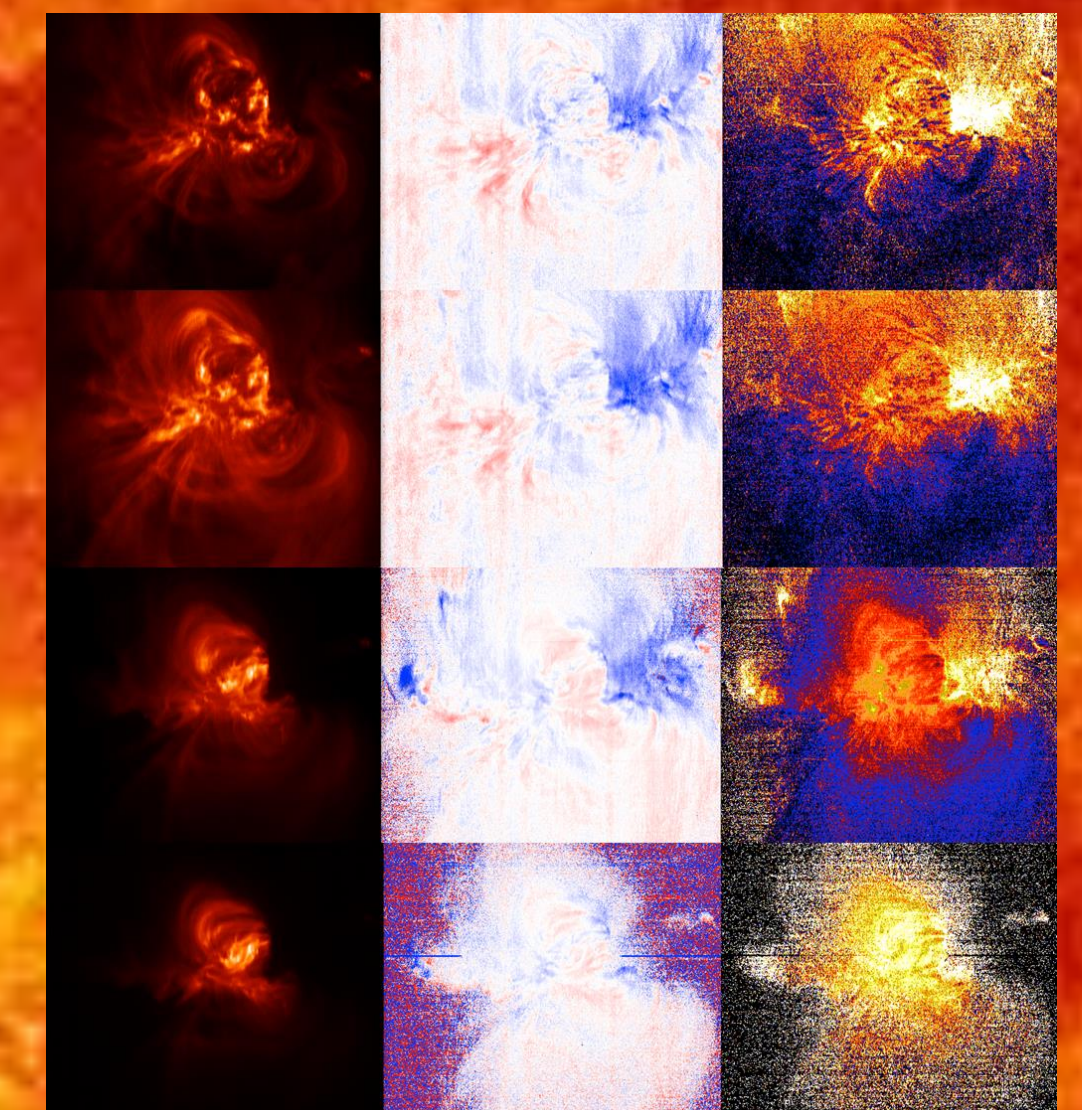
- Figure 5 (top left):** Background conditions for a closed field line – plots of (a) position/height along flux tube, (b) temperature, (c) density, (d) field strength, (e) tube radius, (f) Alfvén speed.
- Figure 6 (top right):** Background conditions for an open field line.
- Figure 7 (left):** Shows how random fluctuations create Alfvén waves – the heating comes in bursts due to the random nature of footpoint motions.

EIS Observations

- The EUV Imaging Spectrometer (EIS) uses a combination of a multilayer and spectrometer in 170-210 Å and 250-290 Å.
- Spectral observations can be used to infer plasma motions.

Figure 8: EIS data, including intensity maps (right), Doppler maps (middle), spectral line width maps (left)

Fe XIII – 202.044 Å
1.6 x 10⁶ K
Fe XII – 192.394 Å
1.0 x 10⁶ K
Fe XV – 284.160 Å
2.0 x 10⁶ K
Fe XVI – 262.980 Å
2.5 x 10⁶ K



Doppler Width

- Sources of line broadening: instrumental, thermal, non-thermal ('microturbulent')
- Total Doppler broadening:

$$v_D = \sqrt{v_{\text{turb}}^2 + \frac{2kT}{m}}$$

- Full Width at Half the Maximum (FWHM) then given by:

$$FWHM = 2\sqrt{2\ln 2} \Delta\lambda_D \approx 2.355 \frac{\lambda}{c} \sqrt{v_{\text{turb}}^2 + \frac{2kT}{m}}$$

Comparisons of Modeling Results with Observations

Closed Field Line

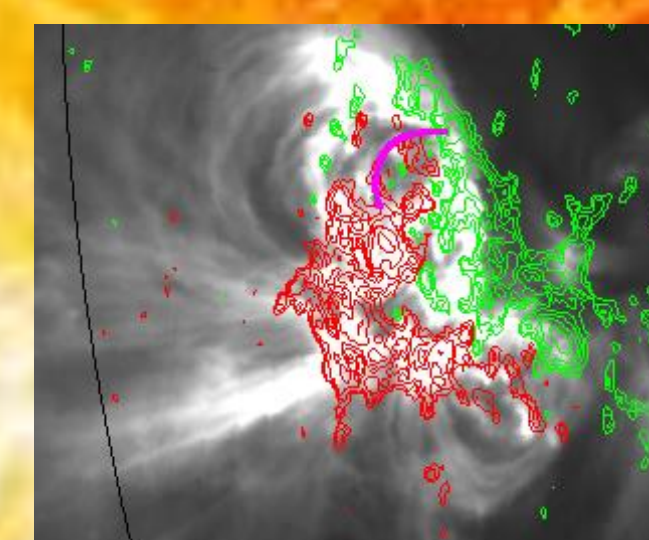


Figure 9: Image of a closed field line

Figure 10: EIS image of the closed field line

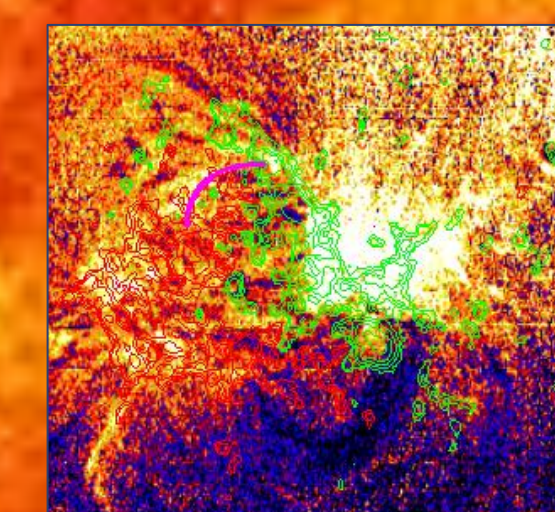


Figure 11 (left): Comparison of observations (black line) with modeling (blue line) for a closed loop

Open Field Line

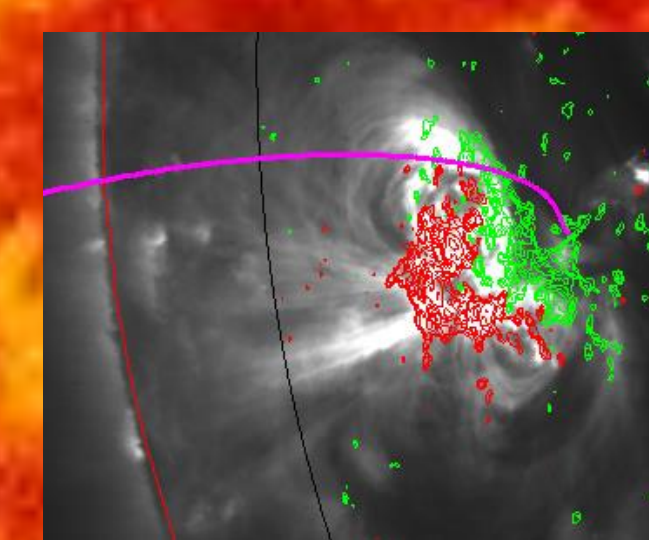


Figure 11: Image of an open field line

Figure 12: EIS image of an open field line

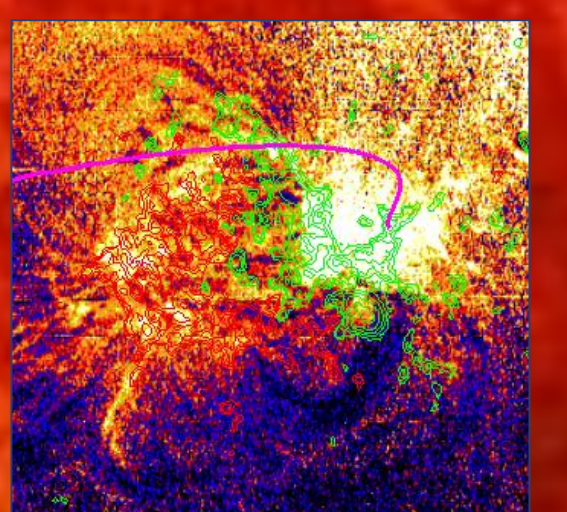


Figure 12 (right): Comparison of observations with modeling for an open loop

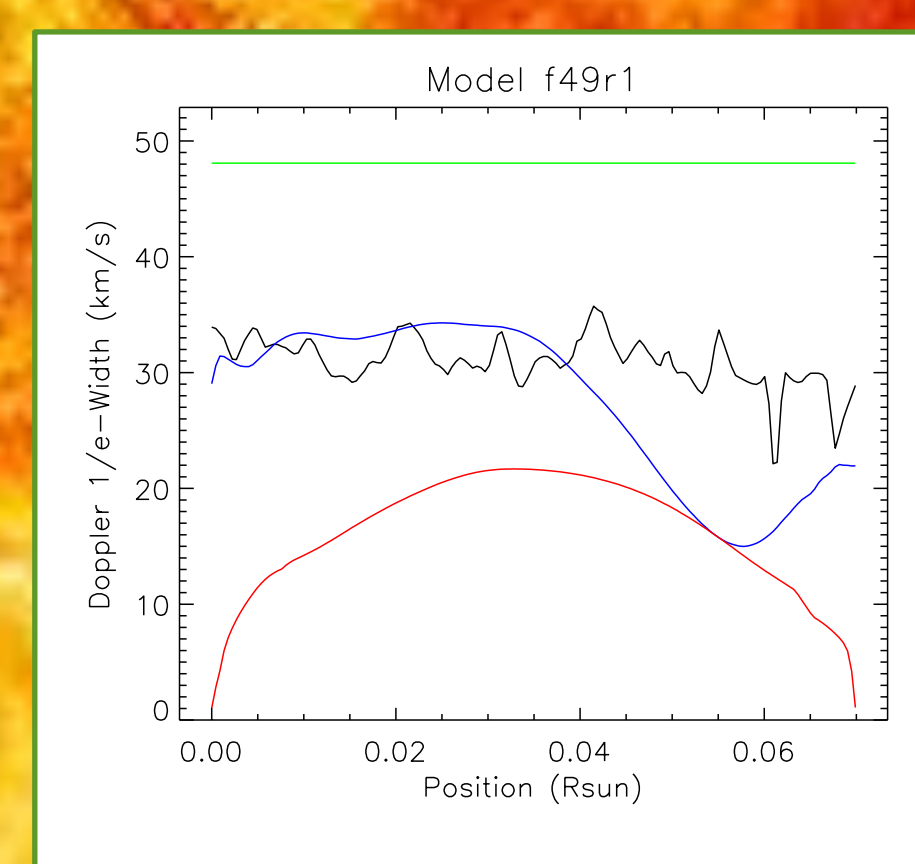


Figure 11 (left): Comparison of observations (black line) with modeling (blue line) for a closed loop

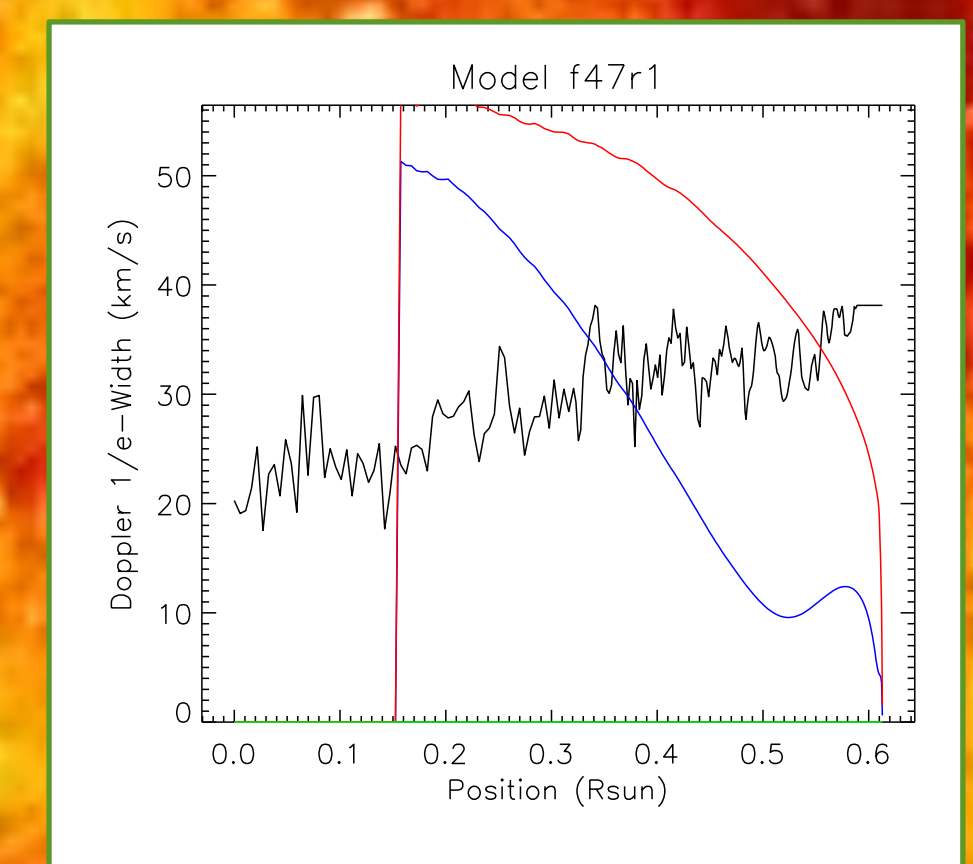


Figure 12 (right): Comparison of observations with modeling for an open loop

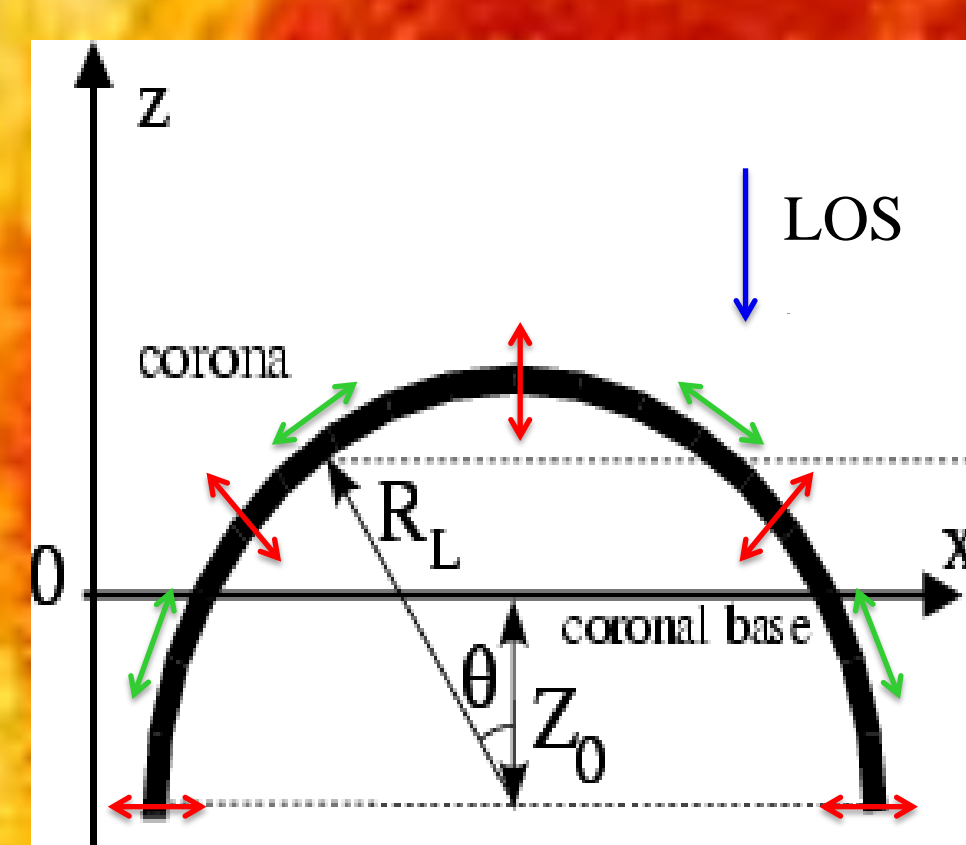


Figure 14: Diagram of a coronal loop showing the parallel velocity, perpendicular velocity and line of sight velocity

- For a closed field line, there is good agreement with observations up until around 0.04 R_{sun} (Fig 11).
- This probably corresponds to the region at which the field line deviates from the observed field lines (fig 10).
- Not such good agreement for open field lines (Fig 12), although the order of magnitude is correct.
- This is probably because the open field lines are further above the surface of the Sun than the EIS observations.

- The LOS velocity (blue line) is calculated from the perpendicular velocity computed from our model (red line) and a constant parallel velocity (green line) as shown in Figure 14.

Conclusions

- In general there is good agreement between modeling results and EIS observations.
- Deviations correspond to regions where the field lines being modeled are at a higher altitude than the observations.
- These difficulties were particularly noticeable in the modeling of open field lines.
- Future work could focus on finding better ways of comparing the open field lines with observations.
- The Alfvén wave model for coronal heating leads to bursts of energy as a result of nonlinear interactions between waves. This is similar to the bursty character of the nanoflare heating.
- With further studies into both models, better observational signatures of both Alfvén waves and nanoflares may be found.

Acknowledgement: This research is supported by the NSF grant for the Solar Physics REU Program at the Smithsonian Astrophysical Observatory (AGS-1263241) and contract SP02H1701R from Lockheed-Martin to SAO.

Reference: Asgari-Targhi, M. & van Ballegouijen, A. A. 2012, ApJ, 746, 81; van Ballegouijen, A. A., Asgari-Targhi, M., Cranmer, S. R., & DeLuca, E. E. 2011, ApJ, 736, 3; Brooks, D. H. & Warren, H. P. 2012, The Astrophysical Journal Letters, 760; Teriaca, L., Banerjee, D. & Doyle, J.G. 1999, Astronomy and Astrophysics, 349, 636-648; Doschek, G. A. 2012, ApJ, 754, 153; Warren, H. P. & Brooks, D. H. 2009, ApJ, 700, 762-773; Aschwanden, M. J. 2005, The Physics of the Solar Corona (Berlin: Springer)